Vietnam Journal of Science and Technology ***63*** *(x) (202x)*

doi:10.15625/2525-2518/18821

Synthesized and properties of g-C_3N_4 bulk and nanosheet from thiourea

Luu Thi Lan Anh[1], Nguyen Quang Truong[1], Nguyen Thi Tuyet Mai[2], Nguyen Cong Tu[1], Le Manh Cuong[3, *]

[1]*Faculty of Engineering Physics, Hanoi University of Science and Technology, 1 Dai Co Viet, Hai Ba Trung, Ha Noi, Viet Nam*

[2]*School of Chemistry and Life Sciences, Hanoi University of Science and Technology, 1 Dai Co Viet, Hai Ba Trung, Ha Noi, Viet Nam*

[3]*Faculty Building Material, Hanoi University of Civil Engineering, 5 Giai Phong, Hai Ba Trung, Ha Noi, Viet Nam*

[*]Emails*: cuonglm@huce.edu.vn*

Received: 5 September 2023; Accepted for publication: 5 June 2025

Abstract. Graphitic carbon nitride (g-C_3N_4) has attracted significant interest due to its stability, low-cost elements, and potential applications in photocatalysis. In this study, g-C_3N_4 bulk was synthesized by thermal polycondensation of thiourea at temperatures ranging from 480 to 550 °C. The influence of calcination temperature on the structural and optical properties of g-C_3N_4 was investigated using XRD, FTIR, SEM, UV-Vis diffuse reflectance, and photoluminescence (PL) analyses. Results showed that g-C_3N_4 synthesized at 520 – 550 °C exhibited high crystallinity with typical (002) and (100) diffraction peaks. FTIR spectra confirmed the presence of triazine units in the structure. Nanosheets of g-C_3N_4 were obtained via thermal oxidation of the bulk in static air, resulting in a porous and expanded morphology. Compared to the bulk, the nanosheets displayed a reduced bandgap energy (from 2.750 eV to 2.625 eV) and blue-shifted PL emission, indicating enhanced separation of photo-induced charge carriers. Lorentz fitting of PL spectra revealed three primary emission centers, related to different transition states. These findings suggest that the synthesized g-C_3N_4 nanosheets possess improved optical properties and could be promising materials for visible-light-driven photocatalytic applications. This work also demonstrates a facile, environmentally friendly route to synthesize g-C_3N_4 materials from thiourea, suitable for scale-up.

Keywords: Graphitic carbon nitride, g-C_3N_4 nanosheet, thiourea precursor, polymerization, photocatalytic materials

Classification numbers: 2.4.2, 2.1.3

1. INTRODUCTION

The graphite carbon nitride (g-C_3N_4) is the most stable allotrope of carbon nitride (C_3N_4) at room temperature [1]. Due to its unique properties such as high thermal and chemical stability,

abundant and low-cost building elements, environmental friendliness, and especially, a suitable electronic structure with band edges straddling the water redox potentials for efficient photocatalytic reactions [2, 6]. The g-C_3N_4 is one of the polymer semiconductors widely used in photocatalysis research because of its outstanding activity for various catalytic reactions, such as the decomposition of organic pollutants [3], producing H_2 and O_2 by splitting water [4] and reducing CO_2 to hydrocarbon fuel [5]. However, the photocatalytic performance of g-C_3N_4 is still restricted by the drawbacks of the high recombination rate of photogenerated electron-hole pairs and limited active sites[7].

Two-dimensional (2D) g-C_3N_4 nanosheets possess large specific surface area, which can not only increase effective reactive sites, and accelerate mass transfer, but also facilitate light absorption and utilization. More importantly, compared with bulk g-C_3N_4, 2D nanosheets can also accelerate photogenerated e-h transfer capability and increase charge lifetime [8 - 14]. Currently, the synthesis of 2D nanosheet structures has more different strategies. Liqiang Jing et al successfully synthesized g-C_3N_4 nanosheets with large surface area via an in-situ way by the developed cyanuric acid-mixed melamine-calcination method [15]. Xiaoqin Zhou et al reported producing g-C_3N_4 nanosheets though thermal exfoliation. The specific surface area of g-C_3N_4 was increased by about 6 times [16]. Superior thin and porous g-C_3N_4 nanosheets were prepared via a two-step thermal polymerization process used to melamine [17]. A rapid and efficient chemical exfoliation method by adding water into concentrated H_2SO_4 suspension of the g-C_3N_4 bulk has been developed for the high-yield production of the g-C_3N_4 nanosheets [18]. The g-C_3N_4 nanosheets were prepared via a simple microwave surface wave plasma technology by using CO_2 gas as the working gas used for urea [19].

The major aim of this work is to synthesize a g-C_3N_4 bulk in a single-step approach via thermal polycondensation using thiourea. The effects of thiourea precursors on g-C_3N_4 formation and properties were investigated. The addition, the g-C_3N_4 nanosheet formed via thermal exfoliation of the g-C_3N_4 bulk in air was investigated.

2. MATERIALS AND METHODS

2.1. Materials

Thiourea was purchased from Sigma-Aldrich with analytical grade purity and used without further purification.

2.2. Synthesis of g-C_3N_4 bulk and nanosheets

The g-C_3N_4 bulk was synthesized by a thermal polymerization method using thiourea precursors. In a typical synthesis, 10 g of thiourea was placed into a porcelain crucible with a cover and heated at temperatures of 480, 500, 520, and 550 °C in air at a rate of 5 °C/min for 2 hours. After cooling to room temperature, the resulting pale-yellow product was collected.

Nanosheets were prepared by thermal exfoliation of the obtained g-C_3N_4 bulk. Specifically, 0.5 g of the bulk sample was placed in an open porcelain crucible and heated at 500 °C in air for 2 hours at a rate of 5 °C/min. The resulting light-yellow powder was collected as g-C_3N_4 nanosheets. Figure 1 presents the scheme synthesized g-C_3N_4 bulk and nanosheet.

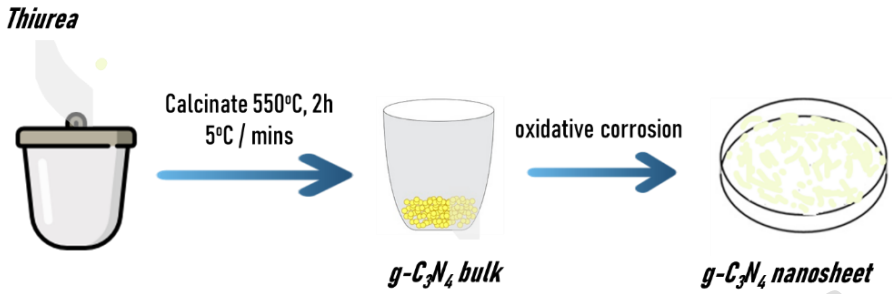

Figure 1. Scheme synthesized g-C_3N_4 bulk and nanosheet.

2.3. Characterization

The crystal structure and phase purity were obtained by using X'pert Pro (PANalytical) MPD with CuK-α1 radiation (= 1.54056 Å) at a scanning rate of 0.03°/2s in the 2θ range from 10° to 70°. The crystal analysis was performed by HighScore Plus software using the ICDD database. FTIR spectra were analyzed using FT/IR-4600typeA (JASCO) with wavenumber from 500 cm^{-1} to 4000 cm^{-1}. The morphology of the samples was investigated with field emission scanning electron microscopy HITACHI S4800 (FESEM, Japan). The Diffusion reflectance of samples was measured in JASCO V-750 using 60 mm Integrating Sphere ISV-922 with a scan rate of 200 nm/min and UV-vis bandwidth of 0.50 nm. The photoluminescence (PL) properties of the g-C_3N_4 samples were measured.

3. RESULTS AND DISCUSSION

3.1. Structural characterization of the material

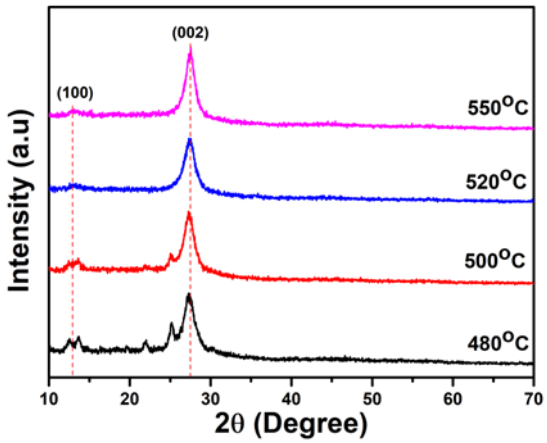

Figure 2. XRD pattern g-C_3N_4 polymerization at temperatures

Figure 2 is the XRD patterns of g-C_3N_4 synthesized by polymerization method from thiourea. The results show that all samples synthesized showed the appearance of two diffraction peaks, in which a strong diffraction peak at angle 2θ = 27.40° corresponds to the diffraction

planes (002), characterizes the superposition of aromatic conjugate systems; Another weaker diffraction peak at 2θ = 12.78° corresponds to the diffraction surface (100), which characterizes the cyclic arrangement of tri-s-triazine or heptazine structural units. Furthermore, the samples synthesized at 500 °C and 480 °C showed the presence of other diffraction peaks indicating incomplete formation of g-C_3N_4 for thiourea. The samples at 520 °C and 550 °C show that the diffraction peaks of g-C_3N_4 are consistent with the standard tag JCPDS number 87-1526 of g-C_3N_4 and previously published results [1, 20].

To investigate the vibrations of organic functional groups, the samples were analyzed using the FTIR method. FTIR spectra of g-C_3N_4 polymerization at temperatures presented in Figure 3 in the range 500 - 4000 cm^{-1}. Typical absorption bands related to the vibration characteristic of g-C_3N_4 appeared in all samples. The NH stretching vibration mode from the surface uncondensed amine groups is assigned to the broadband between 3500 cm^{-1} and 3000 cm^{-1}. Bands between 1700 ~1000 cm^{-1} are assigned to the C=N extension bonds. Prolonged valence oscillations of C-N bonds in aromatic conjugate rings at 1569 cm^{-1} to 1247 cm^{-1}. The two peaks located between 806 and 884 cm^{-1} are derived from the binding of triazine units, indicating that the molecular structure of the prepared g-C_3N_4 consists of triazine units [21]. The results agreed well with the XRD results.

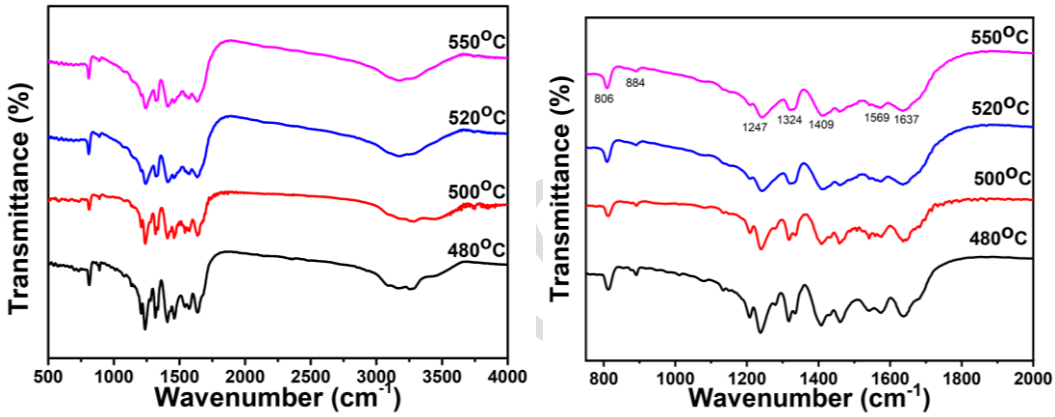

Figure 3. FTIR spectra of g-C_3N_4 calcination at temperatures

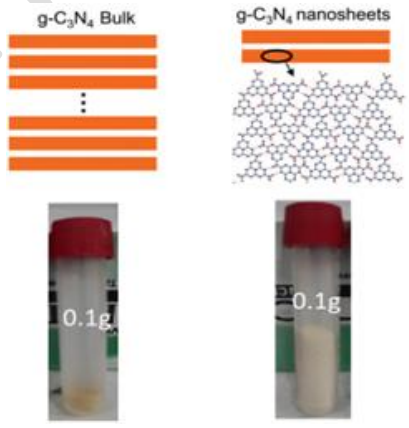

Figure 4. Image of g-C_3N_4 bulk and nanosheet

The image of the g-C_3N_4 bulk and nanosheet is given in Figure 4. The volume of the nanosheets with the same weight is much larger than that of the bulk g-C_3N_4, indicating the fluffy state of the nanosheets.

3.2. Morphological characterization of the material

The morphology of g-C_3N_4 bulk and nanosheets were investigated with FESEM as shown in Figure 5. Compared to their parent bulk material consisting of solid agglomerates with a size of several micrometers (Figure 5a), the representative nanosheets appear as loose and soft agglomerates with a size of tens of micrometers (Figure 5b). This can be easily understood due to the gradual oxidation decomposition of the strands of polymeric melon units in the layers of bulk g-C_3N_4 during etching.

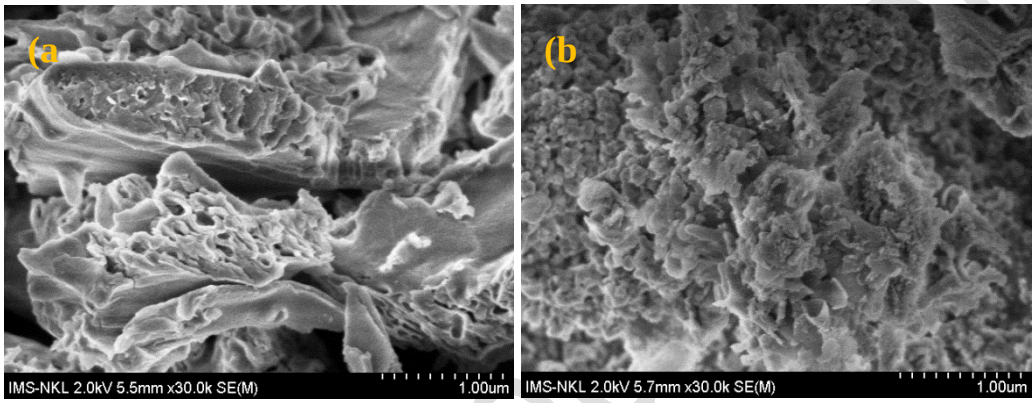

Figure 5. SEM image of g-C_3N_4: (a) bulk and (b) nanosheet

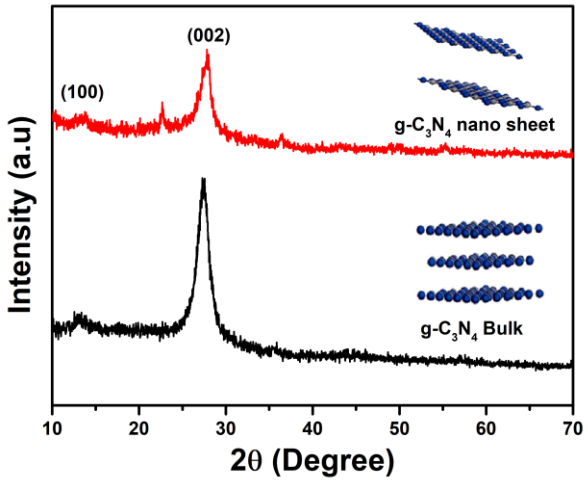

Figure 6. XRD pattern g-C_3N_4 bulk and nanosheet

Figure 6 is the XRD pattern of the sample g-C_3N_4 nanosheet and bulk. The results show that the nanosheet samples show weaker diffraction peak intensity than bulk samples. All samples synthesized from these two precursors showed the appearance of two diffraction peaks,

in which a strong diffraction peak at the angle $2\theta = 27.4^{o}$ corresponds to the diffraction surfaces (002), characterizes the superposition of aromatic conjugate systems; Another weaker diffraction peak at $2\theta = 12.78^{o}$ corresponds to the diffraction surface (100), which characterizes the cyclic arrangement of tri-s-triazine or heptazine structural units. In addition, the nanosheet sample has an additional peak at 23^{o} that can be explained by the presence of O_2 when performing the oxidative 'corrosion' process.

3.3. Optical properties of the material

Figure 7 presents the diffuse reflectance spectrum of the g-C_3N_4 bulk and nanosheet samples. In Figure 7a, it is easy to see that there is a shift in the absorption amplitude towards the short wavelength. Absorption peaks at about 300 - 400 nm characterize the π - π^* transition in conjugated ring systems, including heterocyclic aromatics. The features near 500 nm are due to the n - π^* transition involving free pairs on the N atoms of the triazine ring.

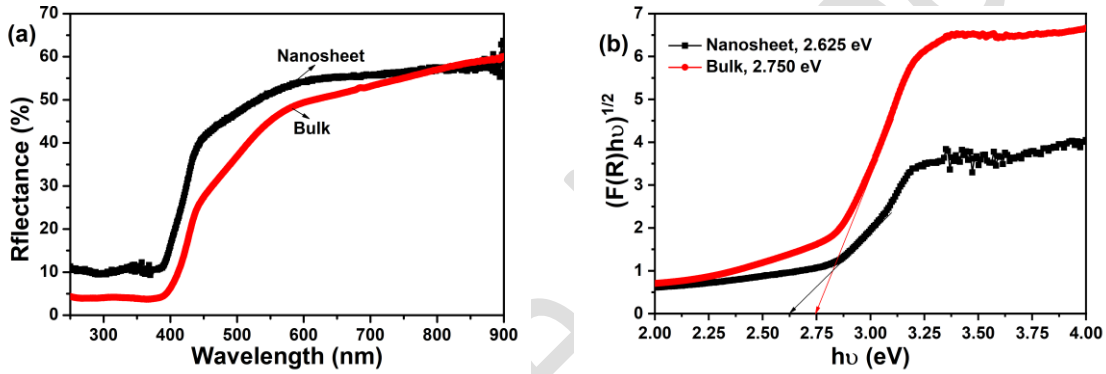

Figure 7. (a) Diffuse reflectance spectra and (b) plot $(F(R)h\nu)^{1/2}$ vs (hν) of g-C_3N_4 bulk and nanosheet.

The optical band gap is extrapolated through the Kubelka-Munk method, where the relationship between incident photon energy hν and the Kubelka-Munk function F(R) follows:

$$(F(R).h\nu = B^*(h\nu - Eg)^n \quad (1)$$

where F(R) is a Kubelka-Munk function determined from the diffuse reflectance R through the formula $F(R) = (1-R)^2/2R$; hν is incident photon energy; and n = 1/2 for direct.

The optical band gap corresponds to a 2.750 eV of the g-C_3N_4 bulk and 2.625 eV of the C_3N_4 nanosheets. The narrowing of the optical band gap could be due to various reasons such as the presence of oxygen vacancies and the surface interaction between g-C_3N_4 nanosheet and H_2S or CS_2.

The emission peak of g- C_3N_4 bulk is around 465 nm, whereas the position of the emission peak shows a shift to about 444 nm for g-C_3N_4 nanosheets, consistent with consistent with the conditions observed in the UV-vis Spectroscopy. The luminescence (PL) spectra of the samples were examined at an excitation wavelength of 340 nm and presented in Figure 8. The g-C_3N_4 bulk shows very strong emission peaks centered at 437 nm, turning to 454nm in the nanosheet. This is consistent with the shift of the absorption band edge after calcination and may be due to the high degree of condensation and filling between the layers in the structure. The PL intensity of the g-C_3N_4 nanosheet is lower than the g-C_3N_4 bulk due to the inhibition of the recombination rate of photo- excited electron-hole pairs, which in turn is ascribed to the thin structure of the

few-layer g-C_3N_4. This inhibition in the recombination of charge carriers is helpful for the enhancement of photocatalyst performance [22,23].

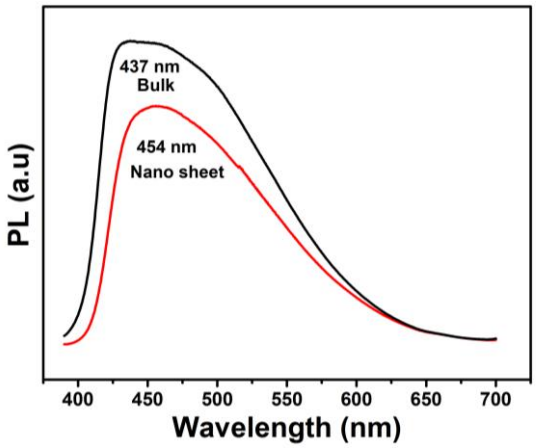

Figure 8. PL spectra of g-C_3N_4 bulk and nanosheet

Lorentz fitting of the PL peaks helps us obtain a clear understanding of the nature and origin of excitons in the g-C_3N_4 bulk and nanosheet. The R^2 value of fit Lorentz results is greater than 0.97, which is very reliable. Three major emission centers have been demonstrated in the fitting and decomposition of the emission spectrum of the g-C_3N_4 samples. Fig. 9a shows the line shape analysis of the g-C_3N_4 bulk, which includes the emission center P1 (430 nm, 2.89 eV), P2 (460 nm, 2.70 eV) and P3 (519 nm, 2.39 eV). In which, the emission center P1 (439 nm, 2.83 eV), P2 (470 nm, 2.64 eV) and P3 (511 nm, 2.43 eV) for g-C_3N_4 nanosheet, investigated. According to the previous PL study of g-C_3N_4, the optical bandgap states of g-C_3N_4 consist of a sp^3 C-N σ band, sp^2 C-N π band and the lone pair (LP) state of the bridge nitride atom, and the P1, P2 and P3 origin from the 3 different pathways of transitions: π*-π, σ*-LP and π*-LP respectively [24]. The emission center of g-C_3N_4 nanosheet is shorter shift. This shift can be explained by the extension of the g-C_3N_4 network. When more heptazine is connected by the amino group, the π states will hybridize into a broad state, causing the bandgap narrowing of the sp^2 C–N clusters.

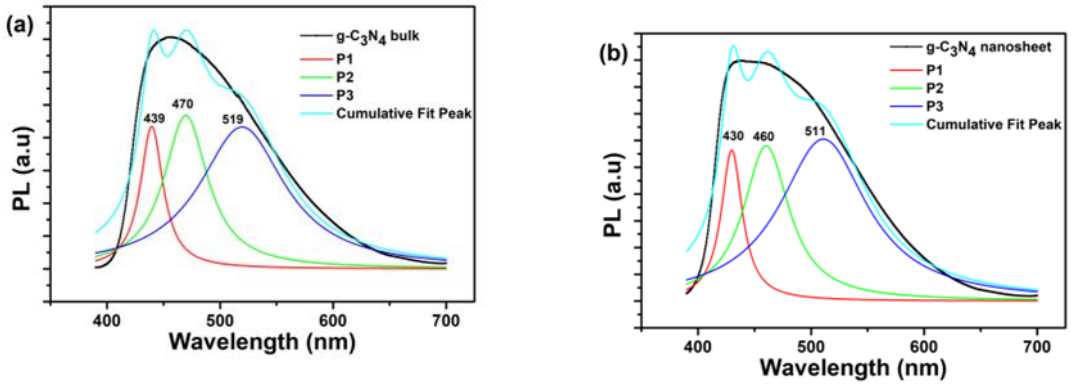

Figure 9. The Lorentz fitting of PL emission spectra of the g-C_3N_4 bulk (a) and nanosheet (b) which indicate 3 major PL peaks (P1, P2 and P3).

4. CONCLUSIONS

Polymeric g-C_3N_4 bulk was successfully synthesized with a facile and environmentally benign approach by directly treating low-cost thiourea in the air at 550 ^oC/2h with a rate of 5 ^oC/min. Thiourea is a better precursor for the synthesis of g-C_3N_4 bulk than a toxic precursor such as dicyandiamide. The g-C_3N_4 bulk has an optical band gap of around 2.750 eV, while the g-C_3N_4 nanosheet has a narrowing optical bandgap of about 2.625 eV, suitable for visible light utilization. The g-C_3N_4 bulk shows very strong emission peaks centered at 437 nm, turning to 437 nm in the nanosheet. The PL intensity of the g-C_3N_4 nanosheet is lower than the g-C_3N_4 bulk due to the inhibition of the recombination rate of photo- excited electron-hole pairs. This work demonstrates a highly valuable facile method to synthesize high-performance g-C_3N_4 polymeric photocatalysts from easily available thiourea for large scale environmental and energetic applications.

Acknowledgements. The research funding from the Ministry of Education and Training (Grant number: B2023-BKA-04) was acknowledged.

Credit authorship contribution statement. Luu Thi Lan Anh: Conceptualization, Supervision, Funding acquisition, Resources, Nguyen Quang Truong: Data curation, Methodology, Investigation, Writing-Original Draft, Nguyen Thi Tuyet Mai: Methodology, Investigation, Formal analysis, Nguyen Cong Tu: Formal analysis, Data Curation, Methodology, Le Manh Cuong: Supervision, Writing - Review & Editing.

Declaration of competing interest. The authors declare that they have no known competing financial interests or personal relationships that could have appeared to influence the work reported in this paper.

REFERENCES

1. Sohail M., Anwar U., Taha T. A., Qazi H. I. A., Al-Sehemi A. G., Ullah S., Algarni H., Ahmed I. M., Amin M. A., Palamanit A., *et al*. - Nanostructured materials based on g-C_3N_4 for enhanced photocatalytic activity and potentials application: A review, Arab. J. Chem. **15** (2022) 104070. https://doi.org/10.1016/j.arabjc.2022.104070.
2. A. Alaghmandfard., K. Ghandi – A Comprehensive Review of Graphitic Carbon Nitride (g-C_3N_4)-Metal Oxide-Based Nanocomposites: Potential for Photocatalysis and Sensing, Nanomaterials **12** (2022) 12020294. https://doi.org/10.3390/nano12020294.
3. M. Raaja Rajeshwari., S. Kokilavani., S. Sudheer Khan – Recent developments in architecturing the g-C_3N_4 based nanostructured photocatalysts: Synthesis, modifications and applications in water treatment, Chemosphere **291** (2022) 132735. https://doi.org/10.1016/j.chemosphere.2021.132735.
4. S.M. Abu-Sari., W.M.A.W. Daud., M.F.A. Patah., B.C. Ang – A review on synthesis, modification method, and challenges of light-driven H_2 evolution using g-C_3N_4-based photocatalyst, Adv. Colloid Interface Sci. **307** (2022) 102722. https://doi.org/10.1016/j.cis.2022.102722.
5. J. Wang., S. Wang – A critical review on graphitic carbon nitride (g-C_3N_4)-based materials: Preparation, modification and environmental application, Coord. Chem. Rev. **453** (2022) 214338. https://doi.org/10.1016/j.ccr.2021.214338.
6. M. Inagaki., T. Tsumura., T. Kinumoto., M. Toyoda – Graphitic carbon nitrides (g-C_3N_4) with comparative discussion to carbon materials, Carbon N. Y. **141** (2019) 580-607. https://doi.org/10.1016/j.carbon.2018.09.082.

7. A. Balakrishnan., M. Chinthala – Comprehensive review on advanced reusability of g-C_3N_4 based photocatalysts for the removal of organic pollutants, Chemosphere **297** (2022) 134190. https://doi.org/10.1016/j.chemosphere.2022.134190.
8. T. Kashyap., S. Biswas., S. Ahmed., D. Kalita., P. Nath., B. Choudhury – Plasmon activation versus plasmon quenching on the overall photocatalytic performance of Ag/Au bimetal decorated g-C_3N_4 nanosheets, Appl. Catal. B Environ. **298** (2021) 120614. https://doi.org/10.1016/j.apcatb.2021.120614.
9. B. Babu., J. Shim., A.N. Kadam., K. Yoo – Modification of porous g-C_3N_4 nanosheets for enhanced photocatalytic activity: In-situ synthesis and optimization of NH4Cl quantity, Catal. Commun. **124** (2019) 123-127. https://doi.org/10.1016/j.catcom.2019.01.009.
10. Y. Dai., Y. Wang., G. Zuo., J. Kong., Y. Guo., C. Sun., Q. Xian – Photocatalytic degradation mechanism of phenanthrene over plasmonic Ag/Ag_3PO_4/g-C_3N_4 nanocomposite, Chemosphere **293** (2022) 133575. https://doi.org/10.1016/j.chemosphere.2022.133575.
11. H. Shi., Y. Li., X. Wang., H. Yu., J. Yu – Selective modification of ultra-thin g-C_3N_4 nanosheets on the (110) facet of Au/$BiVO_4$ for boosting photocatalytic H_2O_2 production, Appl. Catal. B Environ. **297** (2021) 120414. https://doi.org/10.1016/j.apcatb.2021.120414.
12. M. Heydari., N. Azizi., Z. Mirjafari., M.M. Hashemi – Aluminum anchored on g-C_3N_4 as robust catalysts for Mannich reaction, J. Mol. Struct. **1259** (2022) 132731. https://doi.org/10.1016/j.molstruc.2022.132731.
13. M. Arif., Q. Li., J. Yao., T. Huang., Y. Hua., T. Liu., X. Liu – Enhance photocatalysis performance and mechanism of CdS and Ag synergistic co-catalyst supported on mesoporous g-C_3N_4 nanosheets, J. Environ. Chem. Eng. **5** (2017) 5358-5368. https://doi.org/10.1016/j.jece.2017.10.024.
14. S. Rao., Y. Li., H. Liu., S. Gao., J. Zhao., N. Rahman., J. Li, Y. Zhou, D. Wang, L. Zhang, Q. Liu, J. Yang – Polyethyleneimine induced highly dispersed Ag nanoparticles over g-C_3N_4 nanosheets, Ceram. Int. **47** (2021) 8528-8537. https://doi.org/10.1016/j.ceramint.2020. 11.220.
15. X. Zhang., K. Hu., X. Zhang., W. Ali., Z. Li., Y. Qu., H. Wang., Q. Zhang., L. Jing – Surface co-modification with highly-dispersed Mn & Cu oxides of g-C_3N_4 nanosheets, Appl. Surf. Sci. **492** (2019) 125-134. https://doi.org/10.1016/j.apsusc.2019.06.189.
16. Y. Yan., X. Zhou., P. Yu., Z. Li., T. Zheng – Characteristics, mechanisms and bacteria behavior of photocatalysis with a solid Z-scheme Ag/AgBr/g-C_3N_4 nanosheet in water disinfection, Appl. Catal. A Gen. **590** (2020) 117282. https://doi.org/10.1016/j.apcata.2019.117282.
17. X. Zhang., S.P. Jiang., P. Yang – Bright and tunable photoluminescence from the assembly of red g-C_3N_4 nanosheets, J. Lumin. **235** (2021) 118055. https://doi.org/10.1016/j.jlumin.2021.118055.
18. J. Tong., L. Zhang., F. Li., K. Wang., L. Han., S. Cao – Rapid and high-yield production of g-C_3N_4 nanosheets via chemical exfoliation for photocatalytic H2 evolution, RSC Adv. **5** (2015) 88149-88153. https://doi.org/10.1039/c5ra16988g.
19. X. Chang., S. Xu., D. Wang., Z. Zhang., Y. Guo., S. Kang – Flash dual-engineering of surface carboxyl defects and single Cu atoms of g-C_3N_4 via unique CO_2 plasma

immersion approach, Mater. Today Adv. **15** (2022) 100274. https://doi.org/10.1016/j.mtadv.2022.100274.

20. L. Yang., J. Huang., L. Shi., L. Cao., Q. Yu., Y. Jie., J. Fei., H. Ouyang., J. Ye – A surface modification resultant thermally oxidized porous g-C_3N_4 with enhanced photocatalytic hydrogen production, Appl. Catal. B Environ. **204** (2017) 335-345. https://doi.org/10.1016/j.apcatb.2016.11.047.
21. A. Kumar., S. Singh., M. Khanuja – A comparative photocatalytic study of pure and acid-etched template free graphitic C_3N_4 on different dyes, Mater. Chem. Phys. **243** (2020) 122402. https://doi.org/10.1016/j.matchemphys.2019.122402.
22. J. Zhang., M. Zhang., C. Yang., X. Wang – Nanospherical carbon nitride frameworks with sharp edges accelerating charge collection, Adv. Mater. **26** (2014) 4121-4126. https://doi.org/10.1002/adma.201400573.
23. D. Liu., N. Tong., Z. Zhang., Z. Yang., Y. Wang., F. Li., H. Lin., J. Long., X. Wang – Post-synthetic regulation of the structure, morphology and photoactivity of graphitic carbon nitride, Mater. Des. **114** (2017) 208-213. https://doi.org/10.1016/j.matdes.2016.11.087.
24. A. Sharma., M. Varshney., K.H. Chae., S.O. Won – Mechanistic investigations on emission characteristics from g-C_3N_4, g-C_3N_4@Pt and g-C_3N_4@Ag nanostructures, Curr. Appl. Phys. **18** (2018) 1458-1464. https://doi.org/10.1016/j.cap.2018.08.019.